Optimisation of Characteristics of Patin Fish Oil in Alginate Beads using Central Composite Design-Response Surface Methodology

Muhammad Salahuddin Haris[1,2], Noor Ain Nasuha Noor Azam[1], Alya Alivia Abror[3], Teti Estiasih[3] and Shaiqah Mohd Rus[4]*

[1]Department of Pharmaceutical Technology, Kulliyyah of Pharmacy, International Islamic University Malaysia (IIUM), Jalan Sultan Ahmad Shah, 25200 Kuantan, Pahang, Malaysia

[2]IKOP Pharma Sdn. Bhd., Jalan Sultan Ahmad Shah, 25200 Kuantan, Pahang, Malaysia

[3]Department of Food Science and Biotechnology, Faculty of Agricultural Technology, University Brawijaya, Malang, Indonesia

[4]Department of Pharmaceutical Technology, Faculty of Pharmacy and Health Sciences, Royal College of Medicine Perak, Universiti Kuala Lumpur, 30450 Ipoh, Perak, Malaysia

*Corresponding author (e-mail: shaiqah.rus@unikl.edu.my)

Omega-6 and omega-3 polyunsaturated fatty acids (PUFA), which are beneficial for human health and infant development, are abundant in patin fish. However, consuming it as a staple dish is unpleasant for individuals, especially children. As patin fish oil contained in micrometre size alginate beads would be convenient for children to consume, this study aims to optimise the size and sphericity of the beads. The major parameters, sodium alginate concentration, Tween 80 concentration and dripping flow rate, were investigated. A Central Composite Design (CCD)-Response Methodology Surface (RSM) technique was used to optimise the characteristics of the beads, and 19 formulation runs were performed. The bead size and sphericity index data from each run were gathered and analysed using software. The optimised formulation was validated and found to have insignificant difference ($p>0.05$). The optimised model produced by the program was achieved using a sodium alginate concentration of 3.94 % (w/v), Tween 80 concentration of 3.34 % (v/v), and dripping flow rate of 3.07 mL/min. The optimised beads were consistent in both size and sphericity index, which were 4.566 ± 0.043 mm and 0.933 ± 0.015, respectively. The size of the beads was not impacted by any of these factors. However, the sphericity of the beads was affected by the Tween 80 concentration and flow rate. The beads were proven to be nearly spherical with a non-porous structure, as shown by scanning electron microscope images. It is hoped that these beads could be an alternative approach to deliver patin fish oil for convenient consumption.

Keywords: Patin fish oil; alginate; beads; central composite design; sphericity

Received: October 2023; Accepted: November 2023

The patin fish, or *Pangasianodon hypophthalmus*, is a common striped catfish species consumed by Malaysians. Not only is the meat of the patin valuable, but its oil has enormous potential as a nutritional supplement for the growth and development of children's brains [3, 4], the prevention of cardiovascular diseases [1, 2], and other health concerns [5, 6]. It has a high content of polyunsaturated fatty acids (PUFA), with 11.54 ± 0.04 % of omega-6 and 8.45 ± 0.04 % of omega-3 fatty acids [5]. The omega-3 PUFA, mainly docosahexaenoic acid (DHA) and eicosatetraenoic acid (EPA), are abundant in patin fish oil, at 2.076 % and 1.842 %, respectively [7]. Based on the National Health and Morbidity Survey 2019, there has been an increase in the trend of growth retardation among Malaysian children under 5 years of age. In 2015, 17.7 % children were growth retarded, while the trend increased to 21.8 % in 2019 [8].

Children's growth can be supported by consuming EPA and DHA, which are abundant in patin fish. The recommended daily intake of EPA and DHA is 100 to 200 mg per day for children aged 2 to 6 years old and 200 to 250 mg per day for older children [9]. Consumption of EPA and DHA may be particularly beneficial for people who are deficient, for malnourished children, and for geriatric patients with mild cognitive impairment [10]. It can promote healthy neurological development, maintain the nervous system, delay cognitive ageing, and promote long-term optimal cognition [11]. In general, the human brain is 60 % fat, of which 25 % is DHA. DHA has been shown to be essential for optimal brain growth and function, influencing the activity of numerous neurotransmitters, membrane fluidity, intracellular calcium ion signalling, and ultimately neurons [10].

However, it is inconvenient for children, specifically, to get an adequate amount of EPA and DHA by consuming patin fish. Although patin is a famous local cuisine among Malaysian adults, consuming it frequently may cause Malaysians to lose interest. Logically, one would not be able to get the recommended daily amount of fatty acids by consuming patin fish in their meals. Therefore, it is beneficial to produce patin fish oil in the form of a supplement, which is more convenient for daily consumption. There are many fish oil-based supplements on the market, such as Scott's emulsion, StemLabs Omega-3 Fish Oil, BioLife Omega-3 Fish Oil, Blackmore's Fish Oil and Seven Seas Cod Liver Oil. However, all these products usually use marine fish, not freshwater fish like patin.

Generally, only patin flesh is cooked, while its bones, internal organs such as the liver, and blood, are usually discarded. Thus, the benefits of patin fish cannot be maximised from all its parts: internal organs, flesh, visceral fat, and bones. Encapsulating their oil extracts into beads is one method to make Malaysian patin fish oil easier to take, especially for children, and to provide the maximum benefit from patin fish. The use of alginate as an encapsulating agent for patin fish oil is preferred because of its capacity to absorb water, and its safety as its non-toxic substance derived from brown algae. It is also inexpensive and simple to handle. The food industry has been particularly interested in alginate because of its gelling, stabilising and thickening properties [12]. It mostly consists of the sodium salt of alginic acid, or a combination of polyuronic acids made up of D-mannuronic acid and L-guluronic acid residues [13]. The beads produced would then be characterised in terms of size and sphericity index (SI).

Patin fish oil-alginate beads would also improve the commercial value of the native patin fish. In fact, research on patin fish oil is widespread in Indonesia, but less so in Malaysia. There are researchers who have worked on the characterisation of patin oil and its use in the production of hand cream, but not in the production of beads [14]. Before encapsulation methods are widely used commercially, it is critical to determine the optimal encapsulation techniques. However, most studies do not focus on the encapsulation of patin fish oil. A literature search also revealed that there are many papers on fish oil encapsulation, but no study specifically on patin fish oil encapsulation. Therefore, this study aims to optimise the characteristics of patin fish oil in alginate beads in terms of bead size and sphericity for convenient consumption.

EXPERIMENTAL

Chemicals and Materials

The main material used was patin fish oil (Ranee®, Mekong, Vietnam). Other materials included sodium alginate powder (Mw = 216.12 g/mol) (Sigma-Aldrich®, Darmstadt, Germany), Tween 80 emulsifier (Eva Chem®, Selangor, Malaysia), anhydrous calcium chloride ($CaCl_2$) powder (Merck, Darmstadt, Germany) and 250 mL distilled water. All materials other than the patin fish oil were analytical grade.

METHODOLOGY

Experimental Design

Three parameters were investigated: sodium alginate concentration, Tween 80 concentration and dripping flow rate [15, 16]. The experimental design used in this study was a central composite design (CCD). It was used to conduct a simultaneous assessment of influential parameters influencing the determination of the appropriate size and shape of alginate beads. The total number of runs in the CCD was estimated as $2^k + 2k + n_0$, where k and n_0 were the critical factor and replication counts at the centre point, respectively. When $k = 3$ and $n_0 = 5$, the experiment produced 19 runs in a single block. Table 1 lists the CCD values of several parameters (k) such as sodium alginate concentration (A), Tween 80 concentration (B) and dripping flow rate (C).

Encapsulation Process

Preparation of Sodium Alginate Solution

Sodium alginate solution was prepared in accordance with the concentrations proposed by the CCD determined using Design Expert® version 11 software (Stat-Ease, Inc., Minneapolis, USA) as in Table 1.

Table 1. CCD values of several parameters (k) created by the Design Expert® software.

Parameters	-α	-1	0	+1	+α
A: Sodium alginate concentration (w/v %)	3	3	4	5	5
B: Tween 80 concentration (v/v %)	2	2	3	4	4
C: Dripping flow rate (mL/min)	2	2	3.5	5	5

Sodium alginate powder was weighed and dissolved in 250 mL distilled water. Each solution was stirred at 4000 rpm for 5 minutes using a homogeniser. Then, it was continuously stirred using a magnetic stirrer for an hour to produce a homogenous alginate solution.

Preparation of Emulsion

After the homogeneous sodium alginate solution was prepared, the emulsifier, Tween 80, was added into the solution and continuously stirred by the homogeniser at a speed of 4000 rpm for 2 minutes. Then, 15 % v/v of patin fish oil was added to the mixture and stirring was continued for 3 minutes to produce an oil-in-water (O/W) emulsion. The concentration of Tween 80 added was as proposed by the CCD (Table 1).

Preparation of Patin Fish Oil-Alginate Beads

As the emulsion was prepared, it was set for the dripping process using a peristaltic infusion pump. The pump was equipped with a 10-gauge nozzle, and the distance between the tip and the collector solution was set at a constant distance of 15 cm. A 2 % w/v $CaCl_2$ solution was prepared in 250 mL distilled water. This was used as a cross-linking solution for bead formation. The emulsion was pumped out into the $CaCl_2$ solution at a certain dripping flow rate (Table 1). The released beads were immersed in the $CaCl_2$ solution and stirred using a magnetic stirrer (Gyeonggi-do, Republic of Korea) for 30 minutes. After that, the beads were removed and filtered using a sieve and washed with distilled water until hydrogel beads were produced.

Characterisation of Patin Fish Oil-Alginate Beads

Determination of Bead Size

The bead size was determined by measuring the Ferret's diameter of 30 randomly picked beads from each run. Each bead was then measured at its largest diameter, labelled as d_{max}, and perpendicular to the d_{max}, the smallest diameter was measured and labelled as d_{min}. The Ferret's diameter of each bead was measured with a calibrated vernier calliper. The average values for d_{max} and d_{min} were calculated, and this was taken as the bead size. Design Expert® version 11 software (Stat-Ease Inc., Minneapolis, USA) was employed to find the optimized bead size by using the average values for each run.

Determination of SI of Alginate Beads

The SI value was calculated using equation 1 [17]. Beads with SI values close to one were considered ideal and spherical. Therefore, a lower SI value indicated that the bead shape had a greater degree of deformation.

$$\text{Sphericity Index} = d_{min}/d_{max} \quad \text{(Eq. 1)}$$

where d_{min} and d_{max} were the minimum and maximum diameter of the beads, respectively. The average SI for each run was entered in the Design Expert® version 11 software (Stat-Ease Inc., Minneapolis, USA) to determine the parameter values that would produce an optimum SI.

Optimisation of Bead Size and SI

The average values for bead size and SI that were obtained from all 19 runs were entered into the Design Expert® version 11 software (Stat-Ease Inc., Minneapolis, USA). Using the software, the optimal settings for the three manipulated parameters were generated from the data input of the initial 19 runs to produce optimised alginate beads in terms of size and SI. Optimisation of the bead characteristics for the proposed model was guided by a CCD-RSM approach.

Validation of Proposed Model

The optimised model generated was then validated to ensure its robustness. The model was validated in triplicate by measuring bead size and SI following the methods described previously. All average bead size and SI data were considered as experimental values. To validate the model, the theoretical values for bead size and SI as proposed by the Design Expert® software were compared with the experimental values in triplicate and statistically tested using t-tests. A non-significant difference ($p>0.05$) between the predicted and actual values indicates that the proposed model was robust and could produce beads with consistent characteristics. Beads derived from optimum conditions were characterised in terms of bead size, SI and surface morphology.

Surface Morphology

Before the beads were analysed using scanning electron microscopy (SEM), they were carefully dried. The proper dehydration of alginate beads was performed by rinsing with ethanol solutions of increasing concentration (10 %, 50 %, 70 %, 90 % and 100 %) before being allowed to airdry for 30 minutes at room temperature (25 to 30 °C) [16]. A total of ten alginate beads were randomly selected for surface morphology testing using SEM at 21× magnification.

RESULTS AND DISCUSSION

Optimisation of the Characteristics of Patin Fish Oil in Alginate Beads

Bead Size Analysis

The resulting beads were 3.95 ± 0.53 mm – 5.58 ± 0.33 mm in size (Table 2). The size of the beads is significant as it could affect the release of patin fish oil and consumer acceptance [18]. A smaller

size is better as it increases the resistance of the beads to compressive force and shear stress. A higher resistance minimises the possibility of the beads rupturing and stabilises the core [19]. On the other hand, a smaller bead size may also assist the mass transfer and substrate diffusion of the encapsulated patin fish oil. Several parameters are known to affect bead size production. As proposed by the software, the sodium alginate concentration and the dripping flow rate can significantly affect bead size. This was observed in Runs 12 and 14, where the bead sizes produced were smaller compared to other runs, at 3.691 mm and 3.954 mm. Both runs had the highest sodium alginate concentration, which indicated a more viscous solution, and the highest dripping flow rate.

The calculation results showed that the model suggested by the software program for bead size response was a quadratic model (Equation 3). The statistical analysis was done using analysis of variance (ANOVA), as tabulated in Table 3. Based on Table 2, the average bead size for each of the 19 runs was between 3.691 mm and 4.785 mm. The target bead size was between 4 mm and 5 mm. The Design Expert® software suggested a quadratic polynomial model as the best-fit equation for the patin fish oil-alginate bead size. The significance of the model was indicated by its *F*-value and *p*-value, which were 7.90 and 0.0069, respectively. Based on the ANOVA results, the *F*- value of 6.52 implied that the model was significant.

The model was also considered significant when its *p*-value was less than 0.05. In this model, the combination of alginate concentration and dripping flow rate was found to be a significant term. The other model terms were not significant, with *p*-values greater than 0.1000. Additionally, the "lack of fit *F*-value" of 3.47 indicated it was not significant relative to the pure error. The large "lack of fit *F*-value" implied that there was a 12.57 % chance that it could occur due to noise. The non-significance of the "lack of fit *F*-value" was good as the model was required to fit. Equation 2 shows that the size of the patin fish oil-beads in terms of effective factors could be used to predict the response.

$$Y1 = 4.61 - 0.0769A + 0.0077B + 0.0002C - 0.0565AB - 0.27225AC - 0.017BC - 0.119119\ A2 - 0.111119B2 - 0.140619C2 \quad \text{(Eq. 2)}$$

Where: Y_1 = Bead size, A = Alginate concentration, B = Tween 80 concentration, C = Dripping flow rate.

The analysis also showed that the size of the beads increased with the Tween 80 concentration and emulsion flow rate, which was indicated by a positive constant value. In contrast, the response value decreased as the alginate concentration, the interaction between alginate concentration and Tween 80 concentration, the interaction between alginate concentration and emulsion flow rate, and the interaction between Tween 80 concentration and flow rate of emulsion increased, which was indicated by a negative constant value. The polynomial model equation and 3D contour plot were utilized to determine the optimum bead size with reference to the independent variables that consisted of alginate concentration, Tween 80 concentration, and emulsion flow rate (Figure 1(a – f)).

Figure 1 (a-d) shows that bead size increased with alginate concentration to a certain point, and then decreased. The influence of alginate concentration on bead size was insignificant (p-value = 0.1198). The increase in alginate concentration led to larger beads, presumably due to an increase in emulsion viscosity which leads to a higher surface tension of the emulsion, resulting in a maximum volume to form larger beads. However, the decrease in bead size with certain alginate concentrations may be caused by exorbitant alginate solution viscosities (>500mPa), which makes it difficult to pump and causes deformations in bead shape [20]. The composition of the alginate played a significant role in the creation of alginate beads. The viscosity of the sodium alginate solutions increased as the guluronic acid content (GAC) increased, and made the beads stronger. These alginates caused early gelation during the emulsification step, resulting in a larger bead size with more dispersion [20]. At the same time, the molecular mass of alginates, normally defined by the intrinsic viscosity of the solution, had little effect on the size of the beads.

Bead size increased with Tween 80 concentration to a certain point, then the response decreased. The influence of the Tween 80 concentration variable on bead size was insignificant (p-value = 0.8672). The bead size increased presumably because of a decline in the stability of droplets, such as a coalescence due to the concentration of Tween 80 being insufficient to cover the (inter) surfaces of the dispersed phase, resulting in larger droplets. Meanwhile, higher Tween 80 concentrations lower the surface tension of the emulsion, which leads to smaller particle sizes and facilitates the breakdown of sodium alginate droplets into smaller units [21]. Tween 80 concentration may also influence bead size. Higher concentrations of Tween 80 resulted in the formation of smaller beads [22]. However, based on this experiment, it did not have a significant effect compared to other parameters.

Table 2. Average bead size and SI values measured in 19 runs (n=30).

	Factors			Response	
Std	Alginate concentration (%, w/w)	Tween 80 concentration (%, w/w)	Dripping flow rate (ml/min)	Size (mm)	SI
1	3	2	5	4.48 ± 0.25	0.71 ± 0.10
2	3	4	2	4.13 ± 0.14	0.94 ± 0.05
3	4	3	3.5	4.78 ± 0.27	0.95 ± 0.02
4	4	3	5	4.59 ± 0.21	0.86 ± 0.07
5	4	3	3.5	4.56 ± 0.14	0.94 ± 0.03
6	4	2	3.5	4.48 ± 0.15	0.91 ± 0.05
7	4	3	3.5	4.58 ± 0.13	0.93 ± 0.04
8	5	4	2	4.46 ± 0.14	0.87 ± 0.06
9	4	3	2	4.33 ± 0.12	0.95 ± 0.05
10	3	3	3.5	4.40 ± 0.21	0.87 ± 0.08
11	5	3	3.5	4.56 ± 0.16	0.86 ± 0.06
12	5	4	5	3.69 ± 0.86	0.84 ± 0.09
13	5	2	2	4.39 ± 0.19	0.80 ± 0.11
14	5	2	5	3.95 ± 0.53	0.84 ± 0.09
15	4	3	3.5	4.61 ± 0.16	0.96 ± 0.02
16	4	4	3.5	4.50 ± 0.13	0.95 ± 0.03
17	3	4	5	4.71 ± 0.48	0.74 ± 0.35
18	3	2	2	4.10 ± 0.17	0.87 ± 0.09
19	4	3	3.5	4.54 ± 0.14	0.93 ± 0.04

Table 3. ANOVA for Bead Size.

Source	Sum of Squares	df	Mean Square	F-value	p-value	Description
Model	1.15	9	0.1277	6.38	0.0055	*
A-Alginate concentration	0.0591	1	0.0591	2.95	0.1198	**
B-Tween 80 concentration	0.0006	1	0.0006	0.0296	0.8672	**
C-Flow rate of the emulsion	4×10^{-7}	1	4×10^{-7}	0.0000	0.9965	**
AB	0.0255	1	0.0255	1.28	0.2880	**
AC	0.5930	1	0.5930	29.61	0.0004	*
BC	0.0023	1	0.0023	0.1155	0.7418	**
A^2	0.0388	1	0.0388	1.94	0.1975	**
B^2	0.0337	1	0.0337	1.68	0.2266	**
C^2	0.0540	1	0.0540	2.70	0.1349	**
Residual	0.1802	9	0.0200			
Lack of Fit	0.1437	5	0.0287	3.15	0.1444	**
Pure Error	0.0365	4	0.0091			
Cor Total	1.33	18				

*significant
**not significant

Figure 1 (c – f), shows that bead size increased with the flow rate of the emulsion to a certain point, then decreased. The influence of the flow rate of the emulsion variable on bead size was insignificant (p-value = 0.9965). With a low flow rate, the dripping mode is dominant, which increases the bead size. Yet, a higher flow rate initiates a transition from dripping to jet mode. In jet mode, the bead production rate increased, resulting in a decrease in bead size [23]. The dripping flow rate also influenced the average bead size. An increase in flow rate would increase bead size, and vice versa. A smaller bead size was achievable with increasing flow rates as the frequency of droplet formation also increased [15, 20]. One study explained that an increase in flow rate would increase the frequency of droplet formation, which reduces the surface charge density of the beads and produce larger beads [24].

The interaction between alginate concentration and Tween 80 concentration (AB) showed insignificant results for bead size response (p-value = 0.2880). This was similar to the interaction between Tween 80 concentration and emulsion flow rate (BC), which also showed insignificant results for bead size response (p-value = 0.7418). In comparison, the interaction between alginate concentration and the flow rate of emulsion (AC) was significant towards bead size response (p-value = 0.0004). In Figure 1, an increase in bead size was observed under two conditions: (i) by increasing the flow rate when the alginate concentration was 3 % (w/w), or (ii) by increasing alginate concentration when the flow rate of emulsion was 2 ml/min. However, the maximum bead size was achieved while increasing the flow rate at an alginate concentration of 3 % (w/w). This is indicated by the red colour contour. It occurs with a low flow rate, where the dripping mode is dominant, which leads to an increase in bead size [23]. Increasing the feed rate increases the droplet size at the needle tip, resulting in a decreasing surface charge density, and consequently, an increasing bead diameter. However, with a further increase in the feed rate, the frequency of droplet formation at the needle tip increases while droplet size decreases, resulting in a higher surface charge density that decreases the bead diameter.

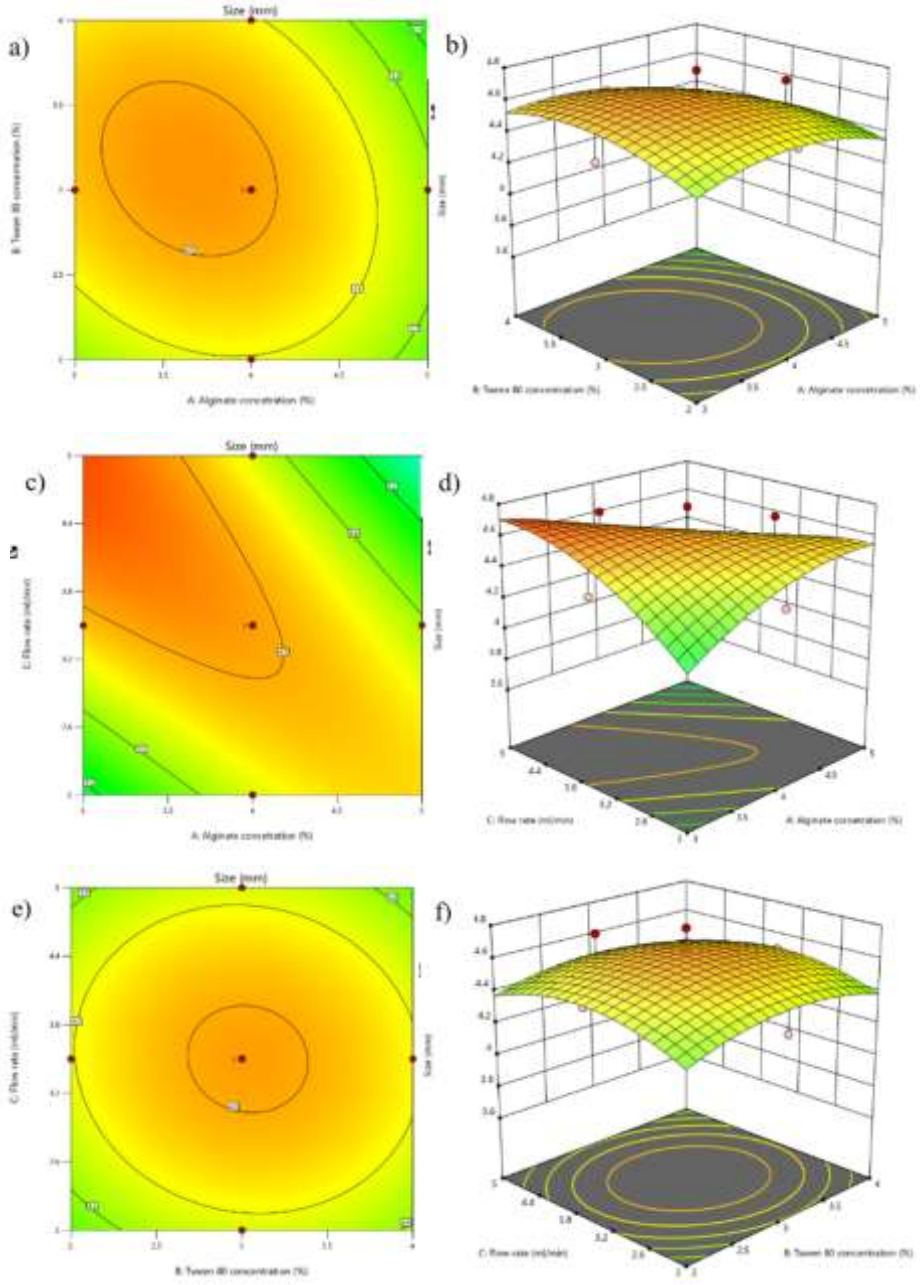

Figure 1. 2D and 3D contour plots of alginate and Tween 80 concentrations (a, b), alginate concentration and flow rate (c, d) and Tween 80 concentration and flow rate (e, f) towards bead size.

SI Analysis

Based on Table 3, the minimum bead SI measured was 0.71, while the maximum value was 0.96. The software suggested a quadratic polynomial model as the best-fit equation for the SI. Based on analysis of variance (ANOVA) tests, the significance of the model was implied by its *F*-value of 63.91 and *p*-value of less than 0.0001 (Table 4). Dripping flow rate and Tween 80 concentration were known to have significant effects on bead sphericity, while sodium alginate concentration alone had a less significant effect. The non-significance of the "lack of fit *F*-value" was good as the model was required to fit. The "lack of fit *F*-value" for the model was not significant relative to the pure error by 1.05. There was a 49.37 % chance that the "lack of fit *F*-value" could happen due to noise. The software proposed Eq. 3 to predict the SI of the beads.

$$Y_2 = 0.942546 + 0.0087A + 0.0205B - 0.044C - 0.005AB + 0.04575AC - 0.014BC - 0.0714794A^2 - 0.00547938B^2 - 0.0359794C^2 \quad \text{(Eq. 3)}$$

For the SI, shape behaviour played a significant part in influencing mechanical and chemical stability. Recent studies confirmed that compared to non-spherical beads, nearly spherical beads generated stronger and firmer gel networks. As a result, the non-spherical ones were more likely to break or crack during manufacturing, releasing the encapsulated ingredient [25]. Besides, the sphericity of the beads could improve the quality desired for nutraceutical and pharmaceutical formulations. An SI of one is optimal, which indicates the bead is perfectly spherical. However, it is difficult to obtain this value; therefore, it is enough for the sphericity value to be close to 1, for which the bead shape can be considered spherical.

The SI of the beads for each run was determined using Eq 1. A rough observation of the patin fish oil-alginate beads showed they were mainly spherical. However, there were also irregular shapes formed, such as a tailing shape, elliptical shape and tear shape. These irregular forms were mainly observed when the dripping flow rate was higher, as in run 1, run 4, run 12, run 14 and run 17. The highest dripping flow rate in this experiment was 5 mL/min, and the lowest was 2 mL/min. Dripping flow rate had a greater effect on the shape of the beads, such that a decrease resulted in increased SI values. However, an increase in the dripping flow rate resulted in difficulties in producing spherical beads, as the solution was continuously flowing from the nozzle into the $CaCl_2$ and not cut. Thus, tailing bead shapes, tear shapes, pear shapes and elliptical shapes were observed. The bead form was not perfectly spherical, and could easily break or crack. In short, lower dripping flow rates produced more precisely rounded beads compared to higher dripping flow rates [25].

Even with a low dripping flow rate, there were other parameters that influenced the sphericity of the beads. Sodium alginate concentration and tween 80 concentration also affected bead sphericity. A low concentration of sodium alginate solution resulted in a lower bead strength and led to tailing shapes occurring [15]. However, even if the ideal shape was formed, keeping the shape proved problematic. From the data obtained, at a sodium alginate concentration of 5 %, the beads formed "a sperm-like shape" while at a 2% concentration of sodium alginate, the beads were weak and easily disrupted when exerted by the calcium drag force [20]. A high concentration of alginate was crucial because $CaCl_2$ could change the alginate conformation if it was less viscous [26]. It could not prevent the bead membrane from being penetrated by Ca ions and disturb the sphere-like shape of the beads. Meanwhile, an increased Tween 80 concentration reduced the alginate-patin fish oil surface tension and prevented production of non-spherical beads [15].

The above equation showed that an average response value for the sphericity factor was 0.942. The equation also showed that the sphericity factor increased as the alginate concentration, Tween 80 concentration, the interaction between alginate concentration, and the flow rate of emulsion variables increased, which was indicated by a positive constant value. In contrast, the value of the response decreased with increases in the flow rate of emulsion, the interaction between alginate concentration and Tween 80 concentration, the interaction between alginate concentration and flow rate emulsion, and the interaction between Tween 80 concentration and flow rate of emulsion variables, which were indicated by a negative constant value. The polynomial model equation and 3D contour plots were utilized to determine the optimum point for the sphericity factor response toward independent variables that consisted of alginate concentration, Tween 80 concentration, and flow rate of emulsion (Figure 2 a-f).

Table 4. ANOVA for SI.

Source	Sum of Squares	df	Mean Square	F-value	p-value	Description
Model	0.0906	9	0.0101	63.91	<0.0001	*
A-Alginate concentration	0.0008	1	0.0008	4.80	0.0561	**
B-Tween 80 concentration	0.0042	1	0.0042	26.68	0.0006	*
C-Flow rate of the emulsion	0.0194	1	0.0194	122.90	<0.0001	*
AB	0.0002	1	0.0002	1.27	0.2890	**
AC	0.0167	1	0.0167	106.30	<0.0001	*
BC	0.0016	1	0.0016	9.95	0.0116	*
A^2	0.0140	1	0.0140	88.63	<0.0001	*
B^2	0.0001	1	0.0001	0.5208	0.4888	**
C^2	0.0035	1	0.0035	22.45	0.0011	*
Residual	0.0014	9	0.0002			
Lack of Fit	0.0008	5	0.0002	1.05	0.4937	**
Pure Error	0.0006	4	0.0002			
Cor Total	0.0920	18				

*significant
**not significant

Figure 2 (a-d) shows that the sphericity factor increased with increasing alginate concentration to a certain point, then decreased. The influence of the alginate concentration variable on the sphericity factor response was insignificant (p-value = 0.0561). The sphericity factor increased with alginate concentration because of increased structural cohesion. The molecular attraction between the polysaccharide (alginate) and the cation (calcium) increased resulting in the immobilization of the encapsulated material [27]. However, the reducing sphericity factor value is likely due to the viscous and sticky nature of the solution. When the emulsion was pumped out through the needle, the high surface tension of the emulsion enabled the beads to adhere at the needle tip. The sticky beads of such a high concentration could not regurgitate a round shape, and as a result, they were cross-linked by calcium ions in the solution [28].

Figure 2 (a, b) and (e, f) showed sharp increases in the value of the sphericity factor along with Tween 80 concentration. The influence of the Tween 80 concentration variable on the sphericity factor response were significant (p-value = 0.0006). An increase in Tween 80 maintains emulsion stability, and provides sufficient time until the emulsion droplets are cross-linked with calcium ions to form spherical beads [21]. Emulsion stability occurs due to a reduction in droplet size. It is attributed to the higher adsorption of surfactants onto oil droplets which result in a more complete coverage of the oil droplet surface, thus preventing the coalescence of some droplets (inter-droplet coalescence) (Ong *et* al., 2015). A surfactant could also produce steric stability as it keeps droplets apart by steric hindrance [29].

An increase in dripping flow rate decreased SI values. The influence of the emulsion flow rate variable in the sphericity factor response was significant (p-value = 0,0001). In the absence of an electric field, a droplet on the tip of a needle develops until it is heavy enough to escape the surface tension of the needle-droplet interface using a gravity force and flow rate. When the flow rate of the emulsion increases, the developed droplets in the tip increases, causing insufficient time to properly construct a Taylor cone at the tip of the needle. Thus, tear-shaped, pear-shaped, and elliptical capsules develop, which reduces the sphericity factor value [20].

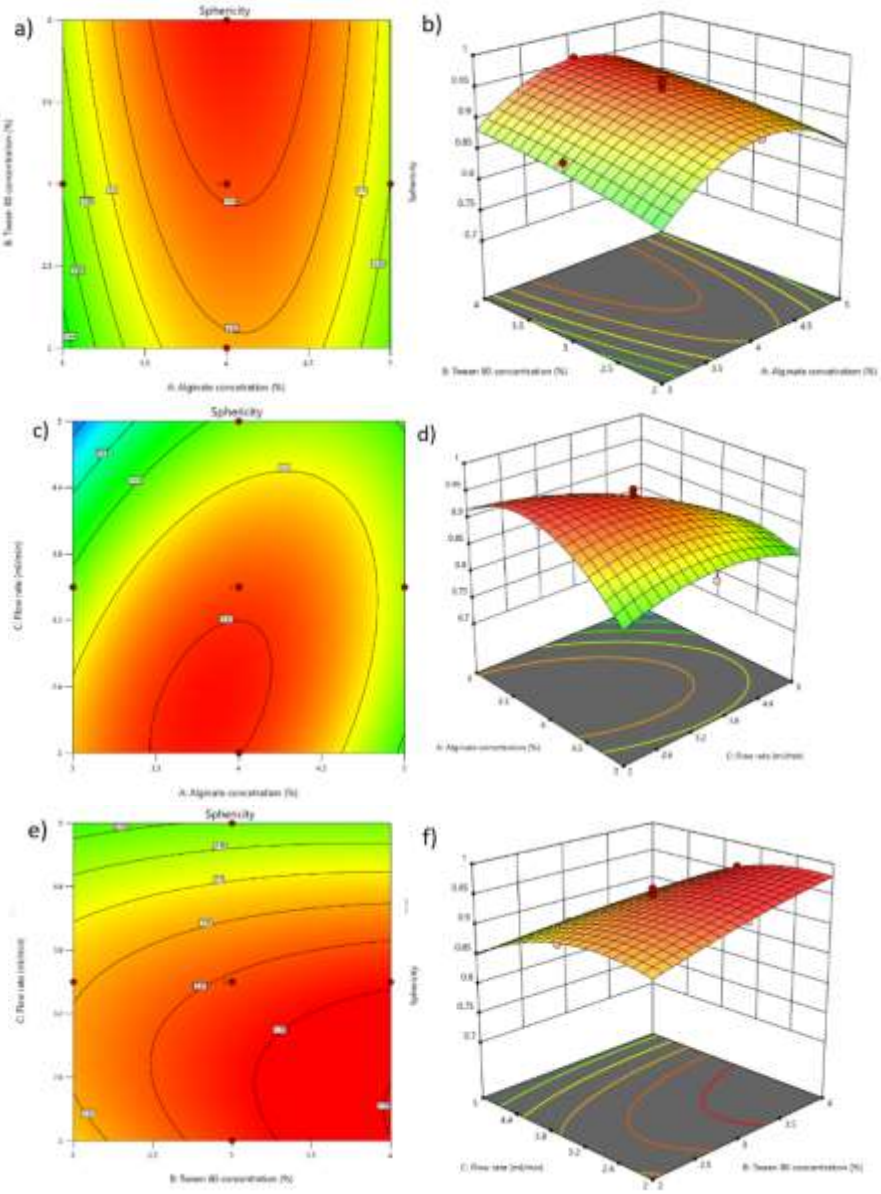

Figure 2. 2D and 3D contour plots for alginate and Tween 80 concentrations (a, b), alginate concentration and flow rate (c, d) and Tween 80 concentration and flow rate (e, f) towards SI.

The interactions between variables are shown in Figure 2. The interaction between alginate concentration and Tween 80 concentration (AB) showed insignificant results toward sphericity factor response (p-value = 0.2890). The interaction between alginate concentration and flow rate of emulsion (AC) showed significant results toward sphericity factor response (p-value = 0.0001). Alginate concentration affects the cohesive structure of the emulsion, which is induced in a bead formation when it forms cross-links with calcium ions. Higher alginate concentrations produce a stronger cohesive structure, yet an exorbitant alginate solution may complicate the detachment of droplets from its tip. The detachment process in the dripping method depends on the gravity force and flow rate of the emulsion forming a Taylor cone [20, 27-28]. Further, the interaction between Tween 80 concentration and flow rate of emulsion (BC) showed significant results toward sphericity factor response (p-value = 0.0116). Tween 80 maintained emulsion stability until the droplets cross-linked with Ca ions, forming spherical beads [21]. The flow rate is a force that is applied to the emulsion. This study assumed that the applied force due to the flow rate of the emulsion affected emulsion stability, which influenced the formation of spherical beads.

Optimisation of Bead Size and SI

After analysis of the bead size and SI data for 19 runs, the Design Expert® software proposed an optimized formulation. Table 5 illustrates the optimised model proposed by the software. This model would produce a bead size of 4.594 ± 0.146 mm and an SI value of 0.960 ± 0.013. The proposed model had a desirability

of 0.909. The desirability value illustrates the program's ability to comply with the desire measured from each predicted response, which is then converted into the desirability value [30]. The value ranges from 0 to 1, where 0 indicates that the response is completely unacceptable, while one indicates the response was the target value. This value increases as the response increases according to the desire of the program, so if the value is close to 1, the optimization accuracy is higher.

Validation of Proposed Model

Verification was carried out after optimisation to test the suitability of the analysis results and parameters. If the predicted value of the response and the results of the verification are not significantly different (p-value > 0.05), the model is considered adequate.

The validation results of the proposed model showed that the average bead size and the SI value were 4.566 ± 0.043 mm and 0.933 ± 0.015, respectively. The results were analysed using paired t-tests and the obtained p-value (p>0.05) for both responses indicated insignificant differences between the predicted and actual values. These results proved that the optimal conditions proposed by the software for alginate concentration, Tween 80 concentration, and flow rate of emulsion were 3.94 (%, w/w), 3.34 (%, w/w) and 3.07 (ml/min), respectively, which produced beads that were consistent in size and spherical in shape.

Surface Morphology

Figure 3 illustrates the surface SEM images of the patin fish oil in alginate beads. The figure shows that a bead produced under optimal conditions is nearly spherical. However, some areas experienced shrinkage, perhaps because the alginate beads were formed by an exogenous method. This method leads to rapid gelation, where the formed particle has a Ca^{2+} concentration gradient which results in a nonhomogeneous gel structure [31]. However, the bead surface was nonporous and smooth indicating the successful encapsulation of the patin fish oil.

Limitations of the Study

The limitations and potential sources of error in this study must be duly acknowledged. It is imperative to recognise that a proper risk evaluation matrix should be done to properly select the critical process parameters that affect the quality attributes of the beads. It must be noted that variability in the quality of raw materials may also contribute to different bead characteristics. Therefore, a quality by design approach should be followed in producing consistent and good quality beads.

Table 5. Validation of proposed model (n=30).

	Factor			Response	
	Alginate Concentration (%)	Tween 80 Concentration (%)	Flow rate of emulsion (ml/min)	Size Bead (mm)	Sphericity Factor
Predicted	3.944	3.343	3.074	4.594 ± 0.146	0.960 ± 0.013
Actual	3.94	3.34	3.07	4.566 ± 0.043	0.933 ± 0.015
Paired t-test (p-value)				0.549**	0.733**

**not significant

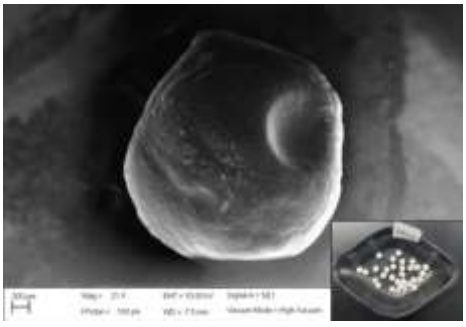

Figure 3. SEM image of an optimised alginate bead containing patin fish oil.

CONCLUSION

The aim of this study was to optimise the characteristics of patin fish oil-alginate bead in terms of bead size and SI. The application of CCD-RSM enhanced the accuracy of the experimental design and provided links between the effects of the parameters and the characteristics of the beads. The optimised conditions for producing consistent size and spherical beads were: a sodium alginate concentration of 3.94 % (w/w), Tween 80 concentration of 3.34 % (v/v) and dripping flow rate of 3.07 mL/min. This study validates our initial hypothesis that bead size and sphericity were affected by these parameters. Specifically, the combination of sodium alginate concentration and dripping flow rate had a substantial impact on bead size, while dripping flow rate and Tween 80 concentration exerted a significant influence on sphericity. Sodium alginate concentration alone had a comparatively modest effect on bead sphericity. These findings provide valuable data to other researchers on the encapsulation of patin fish oil under optimum conditions. To maximise the full potential of this study, future work including stability tests, encapsulation efficiency, swelling studies and compression testing should be performed, so that the many benefits and high commercial value of patin fish oil may be fully utilised.

ACKNOWLEDGEMENTS

The authors would like to thank the Ministry of Higher Education Malaysia for funding this study (grant number: PRGS/1/2021/SKK07/UIAM/02/1).

Conflict of interest

There were no conflicts of interest in the present study. All funding sources of this study are mentioned in the acknowledgements.

REFERENCES

1. Yi, T., Li, S. M., Fan, J. Y. (2014) Comparative analysis of EPA and DHA in fish oil nutritional capsules by GC-MS. *Lipids in Health and Disease*, **13**, 190.

2. Gao, H., Geng, T., Huang, T., Zhao, Q. (2017) Fish oil supplementation and insulin sensitivity: A systemic review and meta-analysis. *Lipids in Health and Disease*, **16**, 131.

3. Ramaswami, R. (2016) Fish oil supplementation in pregnancy. *The New England Journal of Medicine*, **375**, 2599–2601.

4. Hansen, S., Strøm, M., Maslova, E., Dahl, R., Hoffman, H. J., Rytter, D. Bech, B. H., Henriksen, T. B., Granstrom, C., Halldorsson, T. I., Chavarro, J. E., Linneberg, A., Olsen, S. F. (2017) Fish oil supplementation during pregnancy and allergic respiratory disease in the adult offspring. *Journal of Allergy and Clinical Immunology*, **139**, 104-111.

5. Muhamad, N. A. & Mohamad, J. (2012) Fatty Acids Composition of Selected Malaysian Fishes. *Sains Malaysiana*, **41(1)**, 81–94.

6. Ikhsan, A. N., Irnawati, I., Lestari, L. A., Erwanto, Y., Rohman, A. (2022) Simultaneous analysis of patin fish oil (*Pangasius micronemus*) and bandeng (*Chanos chanos*) fish oil using FTIR spectroscopy and chemometrics. *Food Research*, **6**, 262–268.

7. Putri, A., Rohman, A. Riyanto, S. (2019) Comparative study of fatty acid profiles in patin (*Pangasius micronemus*) and gabus (*Channa striata*) fish oil and its authentication using FTIR spectroscopy combined with chemometrics. *International Journal of Applied Pharmaceutics*, **11**, 55–60.

8. National Health and Morbidity Survey (NHMS) (2019) Institute of Public Health, National Institutes of Malaysia, Ministry of Health Malaysia, Kuala Lumpur.

9. Martínez, M. I., Alegre, A., Cauli, O. (2020) Omega-3 long-chain polyunsaturated fatty acids intake in children: The role of family-related social determinants. *Nutrients*, **12**, 3455.

10. Mostafa, G. A. and Al-Ayadhi, L. Y. (2015) Reduced levels of plasma polyunsaturated fatty acids and serum carnitine in autistic children: Relation to gastrointestinal manifestations. *Behavioral and Brain Functions: BBF*, **11**, 4.

11. Rahmawaty, S., Charlton, K., Lyons-Wall, P., Meyer, B. J. (2017) Development and validation of a food frequency questionnaire to assess omega-3 long chain polyunsaturated fatty acid intake in Australian children aged 9–13 years. *Journal Human Nutritional Diet*, **30**, 429–438.

12. Goh, C. H., Heng, P. W. S., Chan, L. W. (2012) Alginates as a useful natural polymer for microencapsulation and therapeutic applications. *Carbohydrate Polymers*, **88**, 1–12.

13. Etchepare, M. D. A., Barin, J. S., Cichoski, A. J., Jacob-Lopes, E., Wagner, R., Fries, L. L. M., Menezes, C. R. D. (2015) Microencapsulation of probiotics using sodium alginate. *Ciência Rural*, **45**, 1319-1326.

14. Shabanikakroodi, S. (2014) *Characterization of oil from liver and visceral fats of patin (Pangasianodon hypophthalmus sauvage) and its use in hand cream preparation* (Doctoral dissertation, Universiti Putra Malaysia).

15. Azhar, M. F., Haris, M. S., Mohamad, I., Ismadi, M. N. S., Yazid, A. A. H., Rahman, S. R., Azlan, N. H. (2021) Optimisation of alginate-pectin bead formulation using central composite design guided electrospray technique. *International Food Research Journal*, **28**, 860–870.

16. Mohd Rus, S., Abu Yazid, A. A. H., Mohamad, I., Ismadi, M. N. S. N., Mohd Azlan, N. H., Rahman, S. R., Doolaanea, A. A., Adina, A. B., Haris, M. S. (2020) Screening of electrospray operating parameters in the production of alginate-royal jelly microbeads using factorial design. *Journal of Pharmacy and Bioallied Science*, **12**, S863–S864.

17. Chan, E. S., Lee, B. B., Ravindra, P., Poncelet, D. (2009) Prediction models for shape and size of ca-alginate macrobeads produced through extrusion–dripping method. *Journal of Colloid and Interface Science*, **338**, 63–72.

18. Lee, J. H. (2013) Polyunsaturated fatty acids in children. *Pediatric gastroenterology, hepatology & nutrition*, **16**, 153–161.

19. Valente, J. F. A., Dias, J. R., Sousa, A., Alves, N. (2019) Composite central face design - An approach to achieve efficient alginate microcarriers. *Polymers*, **11**, 1949.

20. Anani, J., Noby, H., Zkria, A., Yoshitake, T., ElKady, M. (2022) Monothetic analysis and response surface methodology optimization of calcium alginate microcapsules characteristics. *Polymers*, **14**, 709.

21. Mokhtari, S., Jafari, S. M., Assadpour, E. (2017) Development of a nutraceutical nano-delivery system through emulsification/internal gelation of alginate. *Food Chemistry*, **229**, 286-295.

22. Sukmawati, A., Utami, W., Yuliani, R., Da'i, M., Nafarin, A. (2018) Effect of Tween 80 on nano-particle preparation of modified chitosan for targeted delivery of combination doxorubicin and curcumin analogue. In *IOP Conference Series: Materials Science and Engineering*, **311**, 012024.

23. Khorram, M., Mohsen, S., Abdolreza, S., Hamid, M. (2014) Electrospray preparation of propranolol-loaded alginate beads: Effect of matrix reinforcement on loading and release profile. *Journal of Applied Polymer Science*, **132**, 1–9.

24. Partovinia, A., Vatankhah, E. (2019) Experimental investigation into size and sphericity of alginate micro-beads produced by electrospraying technique: Operational condition optimization. *Carbohydrate Polymers*, **209**, 389–399.

25. Voo, W. P., Ooi, C. W., Islam, A., Tey, B. T., Chan, E. S. (2016) Calcium alginate hydrogel beads with high stiffness and extended dissolution behavior. *European Polymer Journal*, **75**, 343–353.

26. Lim, G. P., Lee, B. B., Ahmad, M. S., Singh, H., Ravindra, P. (2016) Influence of process variables and formulation composition on sphericity and diameter of Ca-alginate-chitosan liquid core capsule prepared by extrusion dripping method. *Particulate Science and Technology*, **34**, 681–690.

27. Olloqui, E. J., Castañeda-Ovando, A., Contreras-López, E., Hernandez-Sanchez, D., Tapia-Maruri, D., Piloni-Martini, J., Añorve-Morga, J. (2018) Encapsulation of fish oil into low-cost alginate beads and EPA-DHA release in a rumino-intestinal in vitro digestion model. *European Journal of Lipid Science and Technology*, **120**, 1800036.

28. Shi, P., He, P., Teh, T. K., Morsi, Y. S., Goh, J. C. (2011) Parametric analysis of shape changes of alginate beads. *Powder technology*, **210**, 60–66.

29. Branco, I. G., Sen, K., Rinaldi, C. (2020) Effect of sodium alginate and different types of oil on the physical properties of ultrasound-assisted nano-emulsions. *Chemical Engineering and Processing-Process Intensification*, **153**, 107942.

30. Sahoo, A., Mishra, P. (2014) A response surface methodology and desirability approach for predictive modeling and optimization of cutting temperature in machining hardened steel. *International Journal of Industrial Engineering Computations*, **5**, 407–416.

31. Hu, C., Lu, W., Mata, A., Nishinari, K., Fang, Y. (2021) Ions-induced gelation of alginate: Mechanisms and applications. *International Journal of Biological Macromolecules*, **177**, 578–588.